ELECTRON EXCITATION CROSS SECTIONS FOR THE C II TRANSITIONS $2s^22p\ ^2P^0 \rightarrow 2s2p^2$ 4P, ^2D AND 2_S

M. Zuo[1], Steven J. Smith, and A. Chutjian

Je Propulsion Laboratory, California Institute of Technology, Pasadena, CA 91109

S. S. Tayal

Department of Physics and Center for Theoretical Studies of Physical Systems

Clark Atlanta University, Atlanta, GA 30314

I. D, Williams

Jet Propulsion Laboratory, California Institute of "technology, and Dept. Pure and Applied Physics, The Queen's University, Belfast, UK BT7 1 NN

Abstract

Experimental and theoretical excitation cross sections are reported for the transitions $2s^22p\ ^2P^o \rightarrow 2s2p^2\ ^4P$, 2_D and 2_S in C //. The transition wavelengths (energies) are λ 2324 Å (5.34 eV), λ 1335 Å (9,29 eV), and λ 1036 Å (1 1,96 eV), respectively. Use is made of electron energy-loss and merged-beams methods. The energy range covered is from below each threshold (4-1 1 eV) to 22-25 eV. As in previous work with O //, care was taken to assess and minimize the metastable fraction in the C // beam, to account for contributions from nearby energy-loss features, and to collect the full angular range of inelastically-scattered electrons. Comparison is made for each transition between experiment and a new 8-state /?-matrix calculations,

[1] Present Address: Autometric Service Co., Lakewood, CO

PACS Classification Nos.: 34.80 Kw

1. INTRODUCTION

Determination of the physical conditions of ion density, and electron density and temperature in solar and astrophysical objects depends on observing emissions from singly- and multiply-charged ions in the various sources, This is done through an array of sophisticated ground-based observatories, and most dramatically through space-based observations from, for example, the *Hubble* ***Space*** *Telescope* (Johnson ***et al. 1995),*** the ***Extreme Ultraviolet Explorer*** (Appenzeller ***et al. 1995),*** the ***Hopkins Ultraviolet Telescope*** (Blair ***et al. 1992),*** the *Yohkoh* (Sterling ***et al. 1994)*** and *Hinotori* (Doschek 1990) satellites, and the upcoming ***SOHO*** solar mission ***(ESA 1988).*** Optical emissions from C //, especially the ***A 1335*** Å transition, are detected in these and other solar/stellar observations (Cassinelli ***et a/. 1995,*** Sion ***et a/. 1995,*** Brekke 1993, Davidsen 1993, Savage ***et a/. 1991,*** Lennon ***et a/. 1985).*** The emissions are in almost all cases excited through collisional (electron) excitation ---- requiring collision cross sections or strengths; while the downward transitions are controlled ***via*** radiative decay — requiring optical f-values. For a simple high-density, two-level system, the population N_i of level ***i*** can be expressed as (Gabriel & Jordan 1972; Mason & Monsignori-Fossi 1994),

$$N_i = N_e N_g \frac{C(g \rightarrow i)}{A(i \rightarrow g)} , \qquad (1)$$

where N_e is the electron density, N_g the emitter ground-level density, $A(i \rightarrow g)$ the spontaneous radiative decay rate ***i*** to g, and $C(g \rightarrow i)$ the electron collisional rate coefficient for the transition g $\rightarrow i$. The $C(g \rightarrow i)$ in turn are integrals of the collision

strength or excitation cross section over the appropriate electron energy distribution function (usually taken as Maxwellian) (McLaughlin & Bell ***1993).***

A partial energy-level diagram showing the lowest five states of C // is given in Figure 1, Reported herein are the first measurements, combined with new theoretical (I?-matrix) calculations, of solar- and stellar-prominent e-C // excitations. These excitations are $2s^2 2p\,^2P^0 \rightarrow 2s2p^2\,^4P$ (λ 2324 Å, intercombination), $^2P^0 \rightarrow 2_D$ (λ 1335 Å, allowed), and $^2P^o \rightarrow 2_S$ (λ 1036 Å, allowed), Earlier measurements exist only for the $^2P^0 \rightarrow 2_D$ excitation using inclined beams and absolute photometric calibration of the emitted λ 1335 Å radiation (Lafyatis & Kohl 1987), On the other hand, there exist several calculations of collision strengths using close coupling and allowing for configuration-interaction (Jackson 1973, Lennon et *al* ***1985,*** Luo & Pradhan 1990). We present herein new (8-state) R-matrix close-coupling calculations of both the integral and differential excitation cross sections for the measured transitions,

Experimental details unique to these measurements are given in § 2. The theoretical R-matrix approach is described in § 3, and experimental cross sections compared with theory are given in § 4.

2. EXPERiMENTAL

60° bending magnet, and focused into the interaction chamber immersed in a solenoidal magnet field. Electrons of a chosen energy were

beams (cm^2), and ***u(E)*** the excitation cross section

1 keV-energy C // beam was measured on the central element of a lens system (L2 in Figure 2 of Zuo *et* a/. 1995) as a function of N_2 pressure. The attenuation was measured under two ion-source conditions: one in which the source was run with a high filament current and high anode voltage, and one in which the current and voltage were kept at their lowest levels consistent with stable ion production. A clear discontinuity in slope was seen in the former case, while no detectable break in slope was seen for the low current-voltage case, indicating a metastable fraction of $f \leq 2\%$. Results for the operating mode of low filament current and low anode voltage are shown in Figure 2. An uncertainty of 2% in the final cross section was assigned due to possible metastable contamination (Table 1).

2.2 Overlapping Elastic and Energy-Loss Transitions

Analogous to the effects of overlapping wings in an optical spectrum, a trochoidally-dispersed electron energy-loss feature can contain contribution from electrons that have been elastically-scattered through large scattering angles, and inelastically-scattered in nearby energy-loss transitions. Referring to Fig, 1, excitation to the 2_s state, for example, at a center-of-mass (CM) energy of 13 eV can contain contribution from the edges of the footprint of the $^2P^o \rightarrow {}^2D$ excitation. It can also contain contribution from elastically-scattered electrons.

The methods for treating the elastic and inelastic overlaps have been discussed in Zuo ***et a/. (I 995)*** and Smith *et* a/.

$^2P^o \rightarrow {}^4P$ (intercombination), $^2P^o \rightarrow 2_D$ (allowed), anti $2P" \rightarrow 2_S$ (allowed) signals by electrons elastically-scattered through large angles, l-he maximum uncertainty in the subtraction procedure is *7°/0.*

For convenience we summarize in the following the technique used to calculate the contribution from inelastically-scattered electrons due to nearby energy-loss transitions. Electron trajectory calculations using the SIMION computer code (Dahl & Delmore 1988) were performed to estimate the fraction F of electrons, scattered by competing inelastic processes, which could strike the PSD under a given set of tuning conditions. Only a limited range of laboratory ϑ, φ scattering angles contribute, depending on parameters such as analyzer plate voltages, laboratory (LAB) -to-CM angle transformations, chosen potential on the ['SD retarding grids, and selected region-of-interest (ROI) of the PSD. For a given impact energy, and at each ϑ, the product of the fraction F and the DCS at that ϑ is calculated. The products are summed over all ϑ giving the total adjacent-state contributions at that energy, Simulations were performed at 30 separate energies. A total of approximately 4000 ion trajectories were recorded to build up this overlap information. Based on these results contributions from transitions to adjacent states at other non-calculated energies were interpolated and extrapolated, Overlaps were calculated for the following possibilities:

$2P" \rightarrow 2_D + 2P" \rightarrow 2_S$ contribution to the $2P" \rightarrow 4_P$ signal,

$2P" \rightarrow 4_P + 2P" \rightarrow 2_S$ contribution to the $^2P^o \rightarrow 2_D$ signal,

$2P" \rightarrow 4_P + 2P" \rightarrow 2_D$ contribution to the $^2P^o \rightarrow {}^2S$ signal.

The present 8-state R-matrix DCS calculations as a function of energy for the $^2P^0 \rightarrow$ 4P, ^{2}D, and 2_s transitions are shown in Figures 3, 4, and 5 respectively. In general, the extent of overlapping will depend on the relative magnitudes of the $\sigma(E)$ and the DCS, and on analyzer resolution, which depends on the energy separations of the states involved, The retarding grids allow for better rejection of electrons due to a transition to an adjacent state, if the adjacent state is lower in energy than the upper level of the transition of interest. For example, consider a measurement of the $^2P^o \rightarrow {}^2$D (allowed) transition (see Fig. 1). The 4_P and 2_S adjacent states both can contribute to the 2_D signal, but since the residua energy of the 4_P transition electrons is higher than that of the 2_D transition electrons, one may discriminate between them by the use of retarding grids. The uncertainty introduced in the measured cross sections is estimated to be 2°A (Smi h *et al, 1993).*

2.3 The Electron Mirror

The electron mirror described in Zuo *et al.* (1 995) is used to reflect, into the forward direction, electrons that are inelastically-scattered through laboratory angles in the range $90° < \vartheta \leq 180°$, For a portion of these data, the use of reflectors alone allowed for complete collection over all values of ϑ. For the remaining data, taken before the reflector was installed, a correction ratio R was applied to account for inelastically -backscattered electrons having ϑ

$$R = \frac{2\pi \int_0^{\pi} (d\sigma/d\Omega) \sin\theta \, d\theta}{2\pi \int_0^{\theta_{CM}^{max}} (d\sigma/d\Omega) \sin\theta \, d\theta} \quad (3)$$

where $(d\sigma/d\Omega)$ is the DCS for the relevant transition, and where θ_{CM}^{max} is the maximum CM angle corresponding to scattering at ϑ = 90° in the LAB frame, In this paper the ratio ***R*** is partly determined from theoretical DCS, and also experimentally determined by taking the ratio of a measurement made with the mirror voltage "on" to a measurement make with the mirror voltage "of f," These measurements were made at several energies for the 4P, 2_D and 2_S transitions and yielded good agreement with the ***R*** calculated from the DCS. The final cross section is obtained by multiplying the measured value by the ratio ***R***.

3. COLLISION CALCULATIONS

Electron impact excitation cross sections were calculated for transitions from the ground $2s^2 2p\ ^2P^o$ state of C // to the $2s2p^2$ 4P, ^2D, and ^2S states using the R-matrix method (Barrington e? ***al. 1978),*** Included were the eight LS states ($2s^2 2p$ 'p"; $2s2p^2$ 4p, *D, ^2S,

The 3d, 4s, and 4p orbitals are correlation type and are chosen to improve the energies of the $2s2p^2$ *D, $2s2p^2$ 2_S and $2s2p^2$ 4_P states, respectively. Listed in Table 2 are the parameters of the Slater-type orbitals for the 3s, 3p, 3d, 4s, and 4p functions. A total of 12.1 configurations were used to represent eight C// states. The calculated excitation energies (in eV) relative to the ground state are given in Table 2. They are compared with spectroscopic values (Moore 1949), and with the calculation of Luo & Pradhan (1 989). l-he agreement between the present theoretical and spectroscopic thresholds is better than 2%, except for the $2s2p^2$ 4_P state where the agreement is 5%. Present theoretical results also agree with the calculation of Luo & Pradhan (1 989) who used a scaled Thomas-Fermi-[) irac potential in the optimization procedure (Eissner *et a/. 1974).* "The oscillator strengths for electric-dipole-allowed transitions among the eight *C* // states are listed in Table 3. There is generally good agreement between the length and velocity values of oscillator strengths, The available measured results (Moore 1949) and those from the calculation of Luo & Pradhan (1989) are also listed in the table,

The total wavefunction representing e - C// collision is expanded in terms of the N-electron C// wavefunctions constructed as described above, and the (N+ 1)-electron bound-state-type functions ϕ_j

$$\Psi_k = A \sum_{i,j} c_{ijk} \Phi_i(x_1, x_2,\ldots,x_5; \hat{r}_6\ \sigma_6)\ u_{ij}(r_6) + \sum_j$$

coordinates $r_i \sigma_i$ of the i^{th} electron. The channel functions Φ_j appearing here are eigenstates of L, S and π (parity), formed by coupling a wavefunction of the C // ion to that for the orientational and spin coordinates of the ejected electron. The ϕ_j are six-electron bound-state wavefunctions

4. RESULTS AND DISCUSSION

4.1. Experimental-Theoretical Results for the $^2P^o \rightarrow {}^4P$ (Intercombination) Excitation

Experimental and theoretical cross sections for excitation of the first intercombination 2P" → 4_P λ 2324 Å (5.34 eV) transition are given in Table 5 and shown in Figures 3 and 6. The experimental data are quoted at a 90% confidence level, or 1.7 standard deviations (σ) of the mean, Within the statistical uncertainty, the cross section is zero below threshold, indicating negligible contribution of a $4_P \rightarrow 2_D$ transition (3,95 eV). Shown in Fig. 3 is the theoretical DCS calculated in the range $\vartheta\{0,\pi\}$ at several CM energies between 6,0 and 18.0 eV. Near threshold the DCS is dominated by *s*-wave scattering (essentially isotropic) and becomes more backward-peaked at higher energies. This was also experimentally indicated at 6.0 eV, where the ratio R was measured using the electron mirror, giving close agreement with theory.

Present theoretical calculations have been convoluted with a Gaussian, 250 meV (FWHM) electron energy distribution function. These data are shown as the solid curve in Figure .6, along with calculations of Luo & Pradhan (1990) (dashed curve). There is generally good agreement between the two calculations, and between experiment and calculations, from threshold to the highest energy measured (2.9 x threshold), Some experimental evidence is seen for the resonance minimum at 6.8 eV, especially within smaller *relative* uncertainty limits, but further data at intermediate energies would be needed to establish a clearer resonance profile,

4.2. Experimental-Theoretical Results for the 2P" → ^{2}D (Allowed) Excitation

Experimental and theoretical cross sections for excitation of the first optically-allowed 2P" → 2_D ***λ 1335 Å (9,29*** eV) transition are listed in Table 6 and shown in Figures 4 and 7. The experimental energy range (Figure 7) is threshold to 2.5 x threshold. The DCS in Figure 4 are

4.3. Experimental-Theoretical Results for the 2P" + 2_s(Allowed) Excitation

Experimental and theoretical cross sections for excitation of the second optically-allowed 2P" -> 2_s 1036 Å (1 1.96 eV) transition are listed in Table 7 and shown in Figures 5 and 8. The theoretical DCS has a strong backward component at 12,0 eV, and becomes more forward peaked up to 22,0 eV, the highest energy calculated. This is again consistent with the allowed (resonance) nature of the transition. Experimental measurements of *R* at 14.0 eV confirm the shape of the calculated DCS.

The energy range of the experimental excitation cross sections (Figure 8) is threshold to 2 x threshold. As in the 2P" -> 2_D transition, contributions from the adjacent $^2P^o$ -> 'D and 2P" -> 2_P transitions were calculated based on the respective DCS's and trajectory modeling. These contributions, listed separately in Table 7, were subtracted off, Agreement is again good between the two *R*-matrix calculations and present data.

ACKNOWLEDGEMENTS

M. Z. and 1. D, W. thank the National Academy of Sciences-National Research Council for support at JPL. The theory and supercomputing time was supported by the DoE, Basic Energy Sciences. S. S. 1". acknowledges support from the National Aeronautics and Space Adrninistration under the Planetary Atmospheres Program. The experimental work was carried out at the Jet Propulsion Laboratory, California Institute of Technology, and was supported by NASA.

REFERENCES

Appenzeller, I., Mandel, H., Krautter, J., Bowyer, S., Hurwitz, M., Grewing, M., Kramer, G., & Kappelmann, N. 1995, ***ApJ, 439, L.33***

Barrington, K. A., Burke, P. G., Le Dourneuf, M., Robb, W. D., Taylor, K. T., & Vo Ky Lan 1978, *Comput. Phys. Commun.*, 14, 367

Blair, W. P., Long, K, S., Vancura, O., Bowers, C, W., Conger, S., Davidsen, A, F., Kriss, G, A., Henry, R. B. C. 1992, ***ApJ, 399, 611***

Blum, R. D., & Pradhan, A. K. 1991, *Phys. Rev.* ***A, 44, 6123***

Blum, R. D., & Pradhan, A, K, 1992, *ApJS,* 80, 425

Brekke P. 1993, ***ApJS, 87, 443***

Cassinelli, J. P., Cohen, D. H., MacFarlane, J. J., Drew, J, E., Lynas-Gray, A, E., Hoare, M. G., Vallerga, J. V., Welsh, B. Y., Vedder, P. W., Hubeny, I., & Lanz, T. 1995, ***ApJ,*** 438, 932

Clementi, E. & Roetti, C. 1974, ***At. Data*** *Nucl.* ***Data Jab/es,*** *14*, ***177***

Dahl D. A. & Delmore J. E. 1988, ***Idaho National*** *Engineering* ***Laboratory Report*** *No. EGG-CS-7233* ***Rev, 2*** (unpublished)

Davidsen, A. F, 1993, ***Science,*** 259, 327

Doschek, G, A, 1990, ***ApJS, 73,*** 117

Eissner, W., Jones, M., & Nussbaumer, H. 1974, *Comput. Phys. Commun.,* ***8, 270***

ESA 1988, "The Soho Mission, " ***European Space Agency Report*** *SP-*

Greenwood, J. B., O'Neill, R. W., Hughes, I.G., & Williams, I.D. 1995, unpublished results

Hayes, M. A, & Nussbaumer, H, 1984, *Astron. Astrophys.134,* ***193***

Hibbert, A. 1975, *Comput. Phys. Commun.,* ***9, 14.1***

Jackson, A. R. G. 1972 *J. Phys.* ***B: Atom.*** *Molec. Phys.* ***5, 1.83***

———————---- 1973 ***Mon. Not. Roy.*** *Astron.* ***Sot. 165, 33***

Johnson, H. R., Ensman, L. M., Alexander, D. R., Avrett, E, H., Brown, A., Carpenter, K. G., Eriksson, K., Gustafsson, B., Jorgensen, U. G., Judge, P, D., Linsky, J. L., L.uttermoser, D. G., Querci, F., Querci, M., Robinson, R. D., & Wing, R. F. 1995, ***ApJ,*** 444, 282

Lafyatis, G. P., & Kohl, J. L. 1987, *Phys.* ***Rev. A, 36, 59***

Lennon, D. J., Dufton, P, L., Hibbert, A., & Kingston, A. E. 1985, ***ApJ, 294, 200***

Luo, D. & Pradhan, A. K. 1989, ***J.*** *Phys.* ***b' 22, 3377***

Luo, D., & Pradhan, A. K. 1990, *Phys.* ***Rev. A, 41, 165***

Mason, H. E., & Monsignori Fossi, B, C. 1994, *Astron.* ***Astrophys*** *Rev.,* ***6, 123***

McLaughlin B. M., & Bell K. L, 1993, ***J.*** *Phys. B,* ***26, 1797***

Moore, C. E. 1949, ***Atomic Energy*** *Levels* ***(Circular Nat.*** *Bur. Stds* ***467)*** (Washington, DC: US Govt. Printing Office)

O'Neill, R. W., Hughes, 1, G., & Williams, 1. D. 1991, *Z. Physik* ***D,*** *21,* ***S201***

Savage, B. D., Cardelli, J. A., Bruhweiler, F. C., Smith, A. M., Ebbets, D. C., & Sembach, K. R. 1991, ***ApJ, 377, L53***

Sion, E, M., Cheng, F. H., Long, K, S., Szkody, 1'., Gilliland, R, L., Huang, M, &

Hubeny, I. 1995, *ApJ, 439*, 957

Smith, S.J., Chutjian, A., Mitroy, J., Tayal, S. S., Henry, R. J.W., Man, K-F., Mawhorter, R. J., & Williams, I.D. 1993, *Phys. Rev. A,* 48, 292

Sterling, A. C., Doschek, G. A., and Pike, C. D. 1994, *ApJ,* 435, 898

Unterreiter, E., & Winter, H. 1991, ***XVII Int.Conf Phys. Electron. Atom. Collisions*** (Brisbane, ACT) Abstracts p. 459

Zuo, M., Smith, S. J., Chutjian, A., Williams, I.D., Tayal, S. S., & McLaughlin, B. M. 1995, *ApJ,* 440, 421

Table 1

Individual and Total-Quadrature Experimental Uncertainties in e-C // Data.

Source of uncertainty	Uncertainty at the 1 σ confidence level (%)
Counting statistics	1,0
Form factor	6.0
Path length	1,0
Electron-current measurement	0.5
Ion-current measurement	0.5
PSD efficiency calibration	2.0
Angular correction *R*	5.0
Overlapping elastic contribution	7.0
Overlapping inelastic contribution	2.0
Metastable fraction	2.0
Dead-time correction[a]	-0.0 +2.0
Total quadrature uncertainty (1 .7σ or 90% CL)	+21% -19'%0

[a] I-his one-sided uncertainty is added linearly to the quadrature combination of the remaining uncertainties,

Table 2

Parameters for the Bound Orbitals Used in the Calculation. Each Orbital is a Sum of the Slater-Type Orbitals.

Orbital	Power of r	Exponent
3s	1	4,78401
	2	1.72231
	3	0.88341
3p	2	1.84036
	3	0.73458
3d	3	0.69838
4s	1	4.72112
	2	1.23801
	3	0.75441
	4	1.65516
4p	2	1.95764
	3	1.95645
	4	0.89554

Table 3

Calculated and Spectroscopic Energies of the Excited States of C// Relative to the Ground State.

State	Energy (present, eV)	Luo & Pradhan (1989)	Spectroscopic (Moore 1949)
1. $2s^2 2p$ $^2P^o$	0,0	0.0	0.0
2. $2s2p^2$ ^4P	5.08	5.16	5.34
3. $2s2p^2$ ^2D	9.35	9.41	9.29
4. $2s2p^2$ ^2S	12.12	12.26	11.96
5. $2s2p^2$ ^2P	13.94	13.99	13.71
6. $2s^2 3s$ ^2S	14.39	14.53	14.44
7. $2s^2 3p$ $^2P^o$	16,22	16.40	16.32
8. $2p^3$ $^4S^o$	17.81	18.01	17.60

Table 4

Oscillator Strengths for Electric-Dipole-Allowed Transitions in C// in Length (f_L) and Velocity (f_V) Formulations.

Transition	Present		Luo & Pradhan (1 989)		Experiment
	f_L	f"	f_L	f_V	(Eissner *et al.* 1974)
$2s^22p\ 2D0 \rightarrow 2s2p^2\ 2_D$	0.125	0.135	0.125	0.127	0.120
$2s^22p\ 2P"+\ 2s2p^2\ 2_s$	0.125	0.136	0.129	0.132	0.128
$2s^22p^2?^0 \rightarrow 2s2p^2\ *P$	0.503	0.515	0.517	0.522	0.485
$2s^22p\ 2P" \rightarrow 2s^23s\ 2_S$	0.011	0.008			
$2s2p^2\ 4_P \rightarrow 2p^3\ ^4s^0$	0.178	0.178	0.184	0.174	0.176
$2s2p^2\ 2_D \rightarrow 2s^22p\ ^2P^o$	0.009	0.017			
$2s2p^2\ 2_S \rightarrow 2s^23p\ ^2P^o$	0.180	0.170			
$2s2p^2\ 2_P \rightarrow 2s^23p\ ^2P^o$	0.0001	0.0003			
$2\ s^23s\ 2_s \rightarrow 2s^23p\ ^2P^o$	0.676	0.511			

Table 5

Experimental and Theoretical (/?-matrix) Cross Sections $\sigma(E)$ for the $^2P^o \rightarrow {}^4P$ (Intercombination) Transition in C//

Experimental				*R*-matrix
Energy (eV)	u(E)	*R*	^2D Contrib.	u(E)
4.0	0.025	below threshold		
5.0	0.105	below threshold		
6.0	0.688	reflector		0.925
6.0	0,813	reflector		0.925
6.0	0.851	1.27		0.925
6.1	0.874	1.28		
6.1	0.880	1.27		
7.0	0,644	1.30		
8.0	0.829	reflector		0.561
8.0	0.783	reflector		0.561
8.6	0.573	1.41		
9.0	0.606	1.44		
9.0	0.788	1.44		
9.4	0.651	1.44	0.025	
9.4	0,851	1.48	0.025	
10.0	0.477	reflector	0.070	0.507
10.3	0,404	1.52	0.092	
10.3	0.529	1.54	0.095	
11.1	0.616	1.55	0.129	
11.9	0.579	1.56	0.138	
12.8	0.428	1.55	0.125	
13.7	0.263	1.54	0.095	
14.1	0.376	1.53	0.080	
14.5	0.262	1.53	0.068	
15.0	0.381	reflector	0.045	
15.4	0.283	1.54	0.025	
16.0			0.245	
18.0			0.188	

Notes: Here and in the following tables the ratio *R* is defined in eq. (3). "Reflector" denotes complete angular collection with the mirror. Units of $\sigma(E)$ and 2_D contribution are 10^{-16} cm^2.

Table 6

Experimental and Theoretical (R-matrix) Cross Sections *u(E)* for the $^2P^o \rightarrow {}^2D$ (Allowed) Transition in C II

Energy (eV)	Experimental u(E)	*R*	4_p Contrib.	2_s Contrib.	R-matrix u(E)
8.6	0.074	below theshold			
9.4	0.657	**1,00**			
10.0					1.02
10.0	1.29	reflector			
10,0	1.14	reflector			
10.0	1.28	reflector			
10.3	1,06	1.22	0.016		
10.3	1,26	1.22	0.014		
10.7	0.953	reflector	0.024		
11.1	1.12	1.26	0.036		
11.5	1.71	1.33	0.045		
12.0					1.02
12.4	0.751	1.33	***0.054***		
12.8	1.37	1,30	0.058	***0.026***	
13.5	1.29	reflector	0.055	0.025	
13.6	1.08	reflector	0.055	0.025	
13.7	0.936	1.30	0.054	0.025	
14.0					0.957
14.5	0.964	1.29	**0.038**	0.024	
15.0	1.30	reflector	***0.026***	0.024	
15.4	1.52	1.28	0.015	0.022	
15.4	0.89	1.28	0.015	0.022	
16.0					0.878
16.3	1.08	1.27	**0**	0.021	
16.3	1.19	1.27	**0**	0.021	
17.1	1.05	1.26	**0**	0.020	
18.0	1.26	1.26	**0**	0.022	
18.0					0.799
18.4	1.28	1.25		**0.025**	
18.9	1.04	1.24		***0.024***	
19.8	0.908	1.22		0.029	
20.0					0.854
21.4	0.793	1.22		0.041	
21.5	0.729	1.22		0.042	
21.5	0.986	1.22		0.044	
21.8	0.852	1.22		0.044	
22.0					0.792
22.4	1.08	1.21	().[]49		
22.7	0.643	1.22	0.054		
23.6	0.84	1.22	0.058		

Table 7

Experimental and Theoretical (R-matrix) Cross Sections $\sigma(E)$ for the $^2P^o \rightarrow {}^2S$ (Allowed) Transition in C II

FIGURE CAPTIONS

Figure 1. **Partial** energy-level diagram for C // showing the $2s^2 2p\ ^2P^0 \rightarrow 2s2p^2\ ^4P$ (intercombination), and $2s^2 2p\ ^2P^0 \rightarrow 2s2p^2\ ^2D$, ^2S, and 2_P (allowed) transitions.

Figure 2. **Attenuation** curve measured for a 1 keV beam of *C //* in N_2. The ion source was run at low filament current and low anode voltage, giving a metastable fraction f = **0.00-0.02.**

Figure 3. **Present theoretical differential cross sections for excitation of the 2P" → $2s2p^2\ 4_P$** transition in *C //* in the 8-state close-coupling approximation. Incident electron energies are indicated on each curve.

Figure 4. Present theoretical differential cross sections for excitation of the 2P" → $2s2p^2\ 2_D$ transition in *C //* in the 8-state close-coupling approximation. Incident electron energies are indicated on each curve.

Figure 5. Present theoretical differential cross sections for excitation of the $^2P^o \rightarrow 2s2p^2\ 2_S$ transition in *C //* in the 8-state close-coupling approxirnation. Incident electron energies are indicated on each curve,

Figure 6. **Experimental (.) and theoretical cross sections [convoluted with a 250** meV (FWHM) resolution: — ___ , present *R*-matrix; - - - - -, Luo & Pradhan (1 990)] for excitation of the $^2P^0 \rightarrow 2s2p^2\ ^4P$ (intercombination) transition in C //.

Figure 7. Experimental (●) and theoretical cross sections [convoluted with a 250 meV (FWHM) resolution: —-———— , present *R*-matrix; - - - - -, Luo & Pradhan (1 990)] for excitation of the 2P" → $2s2p^2\ 2_D$ (allowed) transition in C //. Other experimental data are (□), Lafyatis & Kohl (1 987) — inclined beams, absolute UV photometry; (A), Greenwood *et*

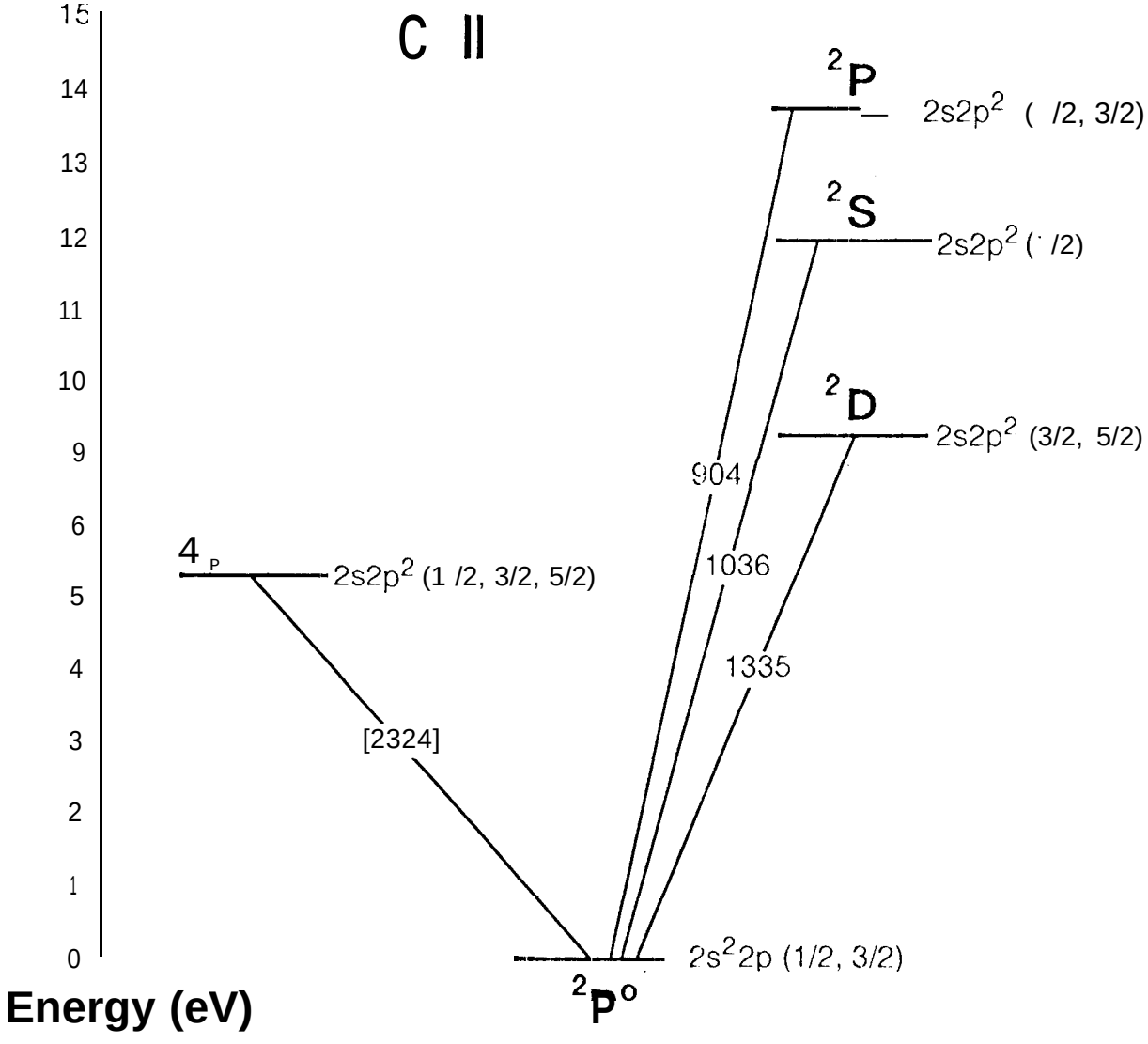
C II
15
14
13
12
11
10
9
6
5
4
3
2
1
0
Energy (eV)
2P
2s2p2 (/2, 3/2)
2S
2s2p2 (/2)
2D
2s2p2 (3/2, 5/2)
4P
2s2p2 (1 /2, 3/2, 5/2)
904
1036
1335
[2324]
2s22p (1/2, 3/2)
2Po

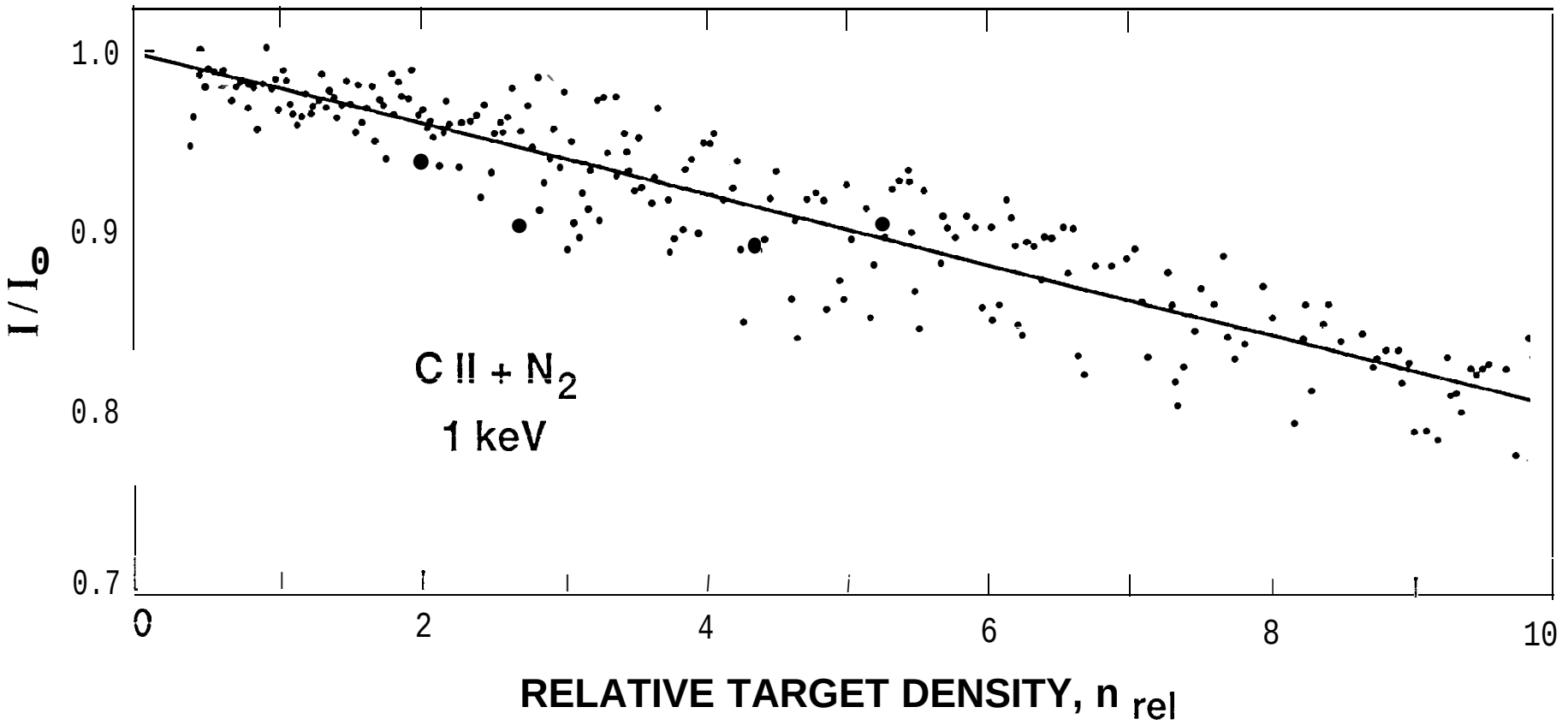
1.0
0.9
0.8
0.7
I / I0
C II + N2
1 keV
0
2
4
6
8
10
RELATIVE TARGET DENSITY, n rel

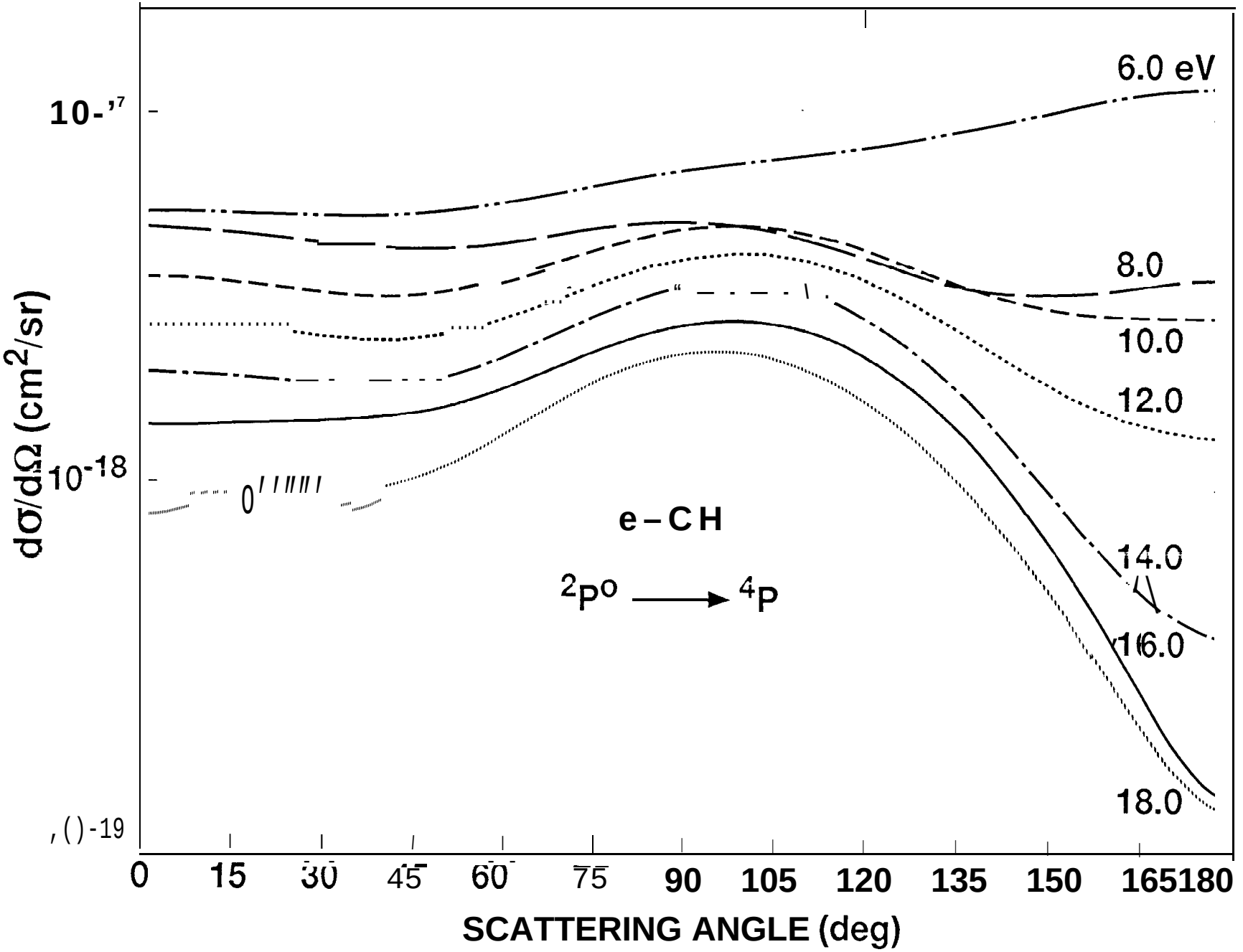
6.0 eV
8.0
10.0
12.0
14.0
16.0
18.0
e – CH
2Po → 4P
dσ/dΩ (cm2/sr)
SCATTERING ANGLE (deg)
0 15 30 45 60 75 90 105 120 135 150 165 180

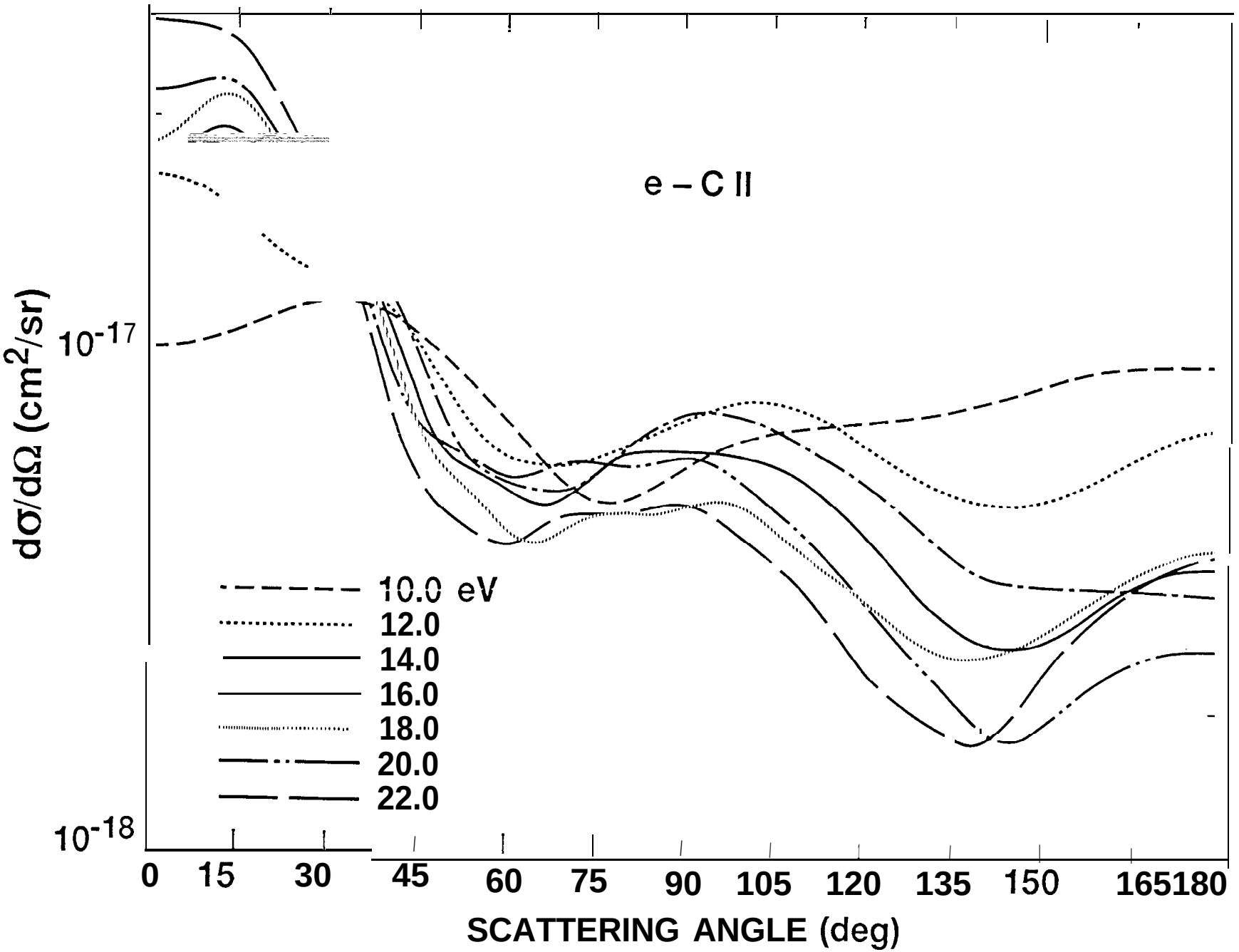
e – C II
dσ/dΩ (cm²/sr)
10⁻¹⁷
10⁻¹⁸
10.0 eV
12.0
14.0
16.0
18.0
20.0
22.0
0
15
30
45
60
75
90
105
120
135
150
165
180
SCATTERING ANGLE (deg)

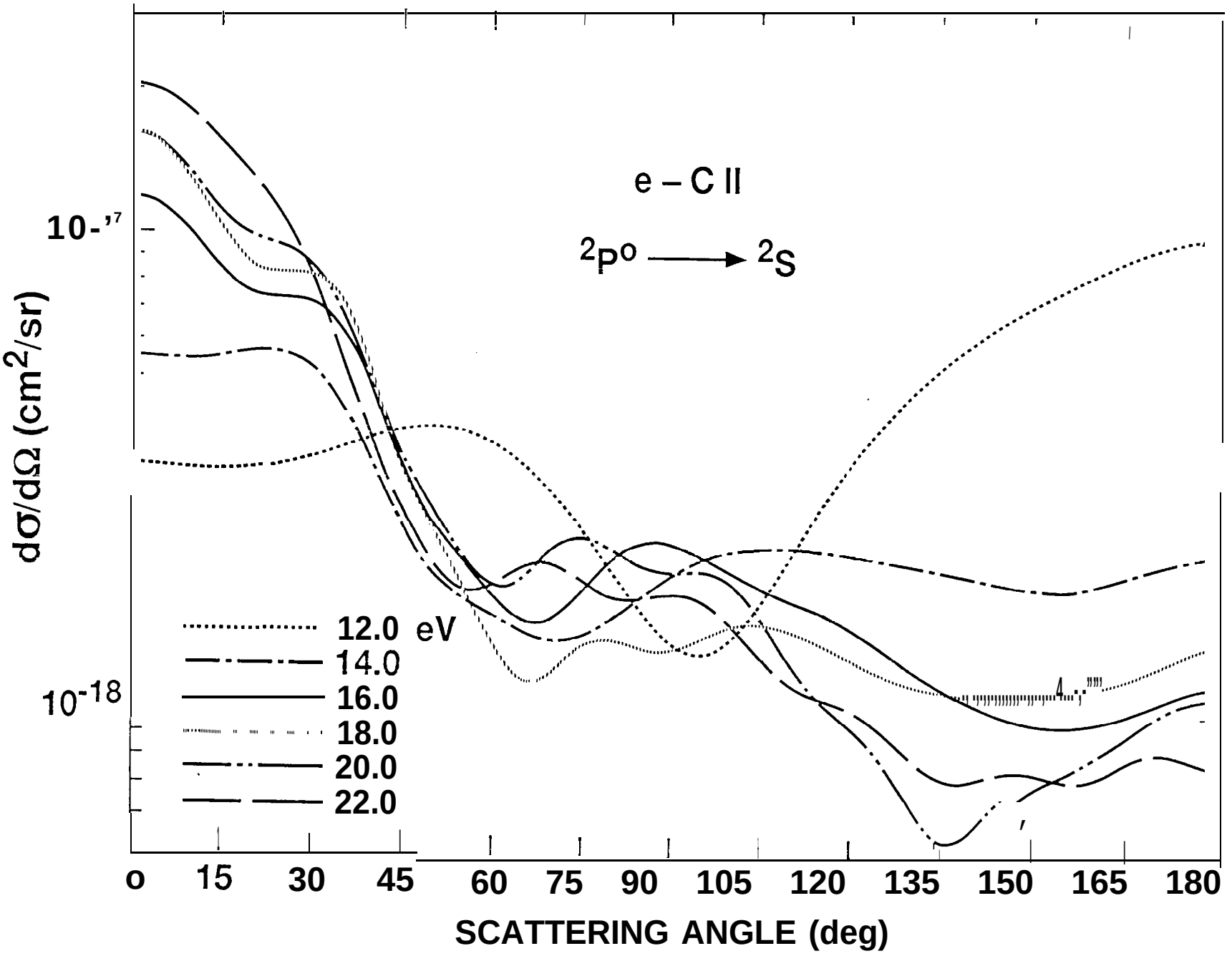
e – C II
$^2P^o \longrightarrow {}^2S$
10^{-17}
10^{-18}
$d\sigma/d\Omega$ (cm^2/sr)
12.0 eV
14.0
16.0
18.0
20.0
22.0
0
15
30
45
60
75
90
105
120
135
150
165
180
SCATTERING ANGLE (deg)

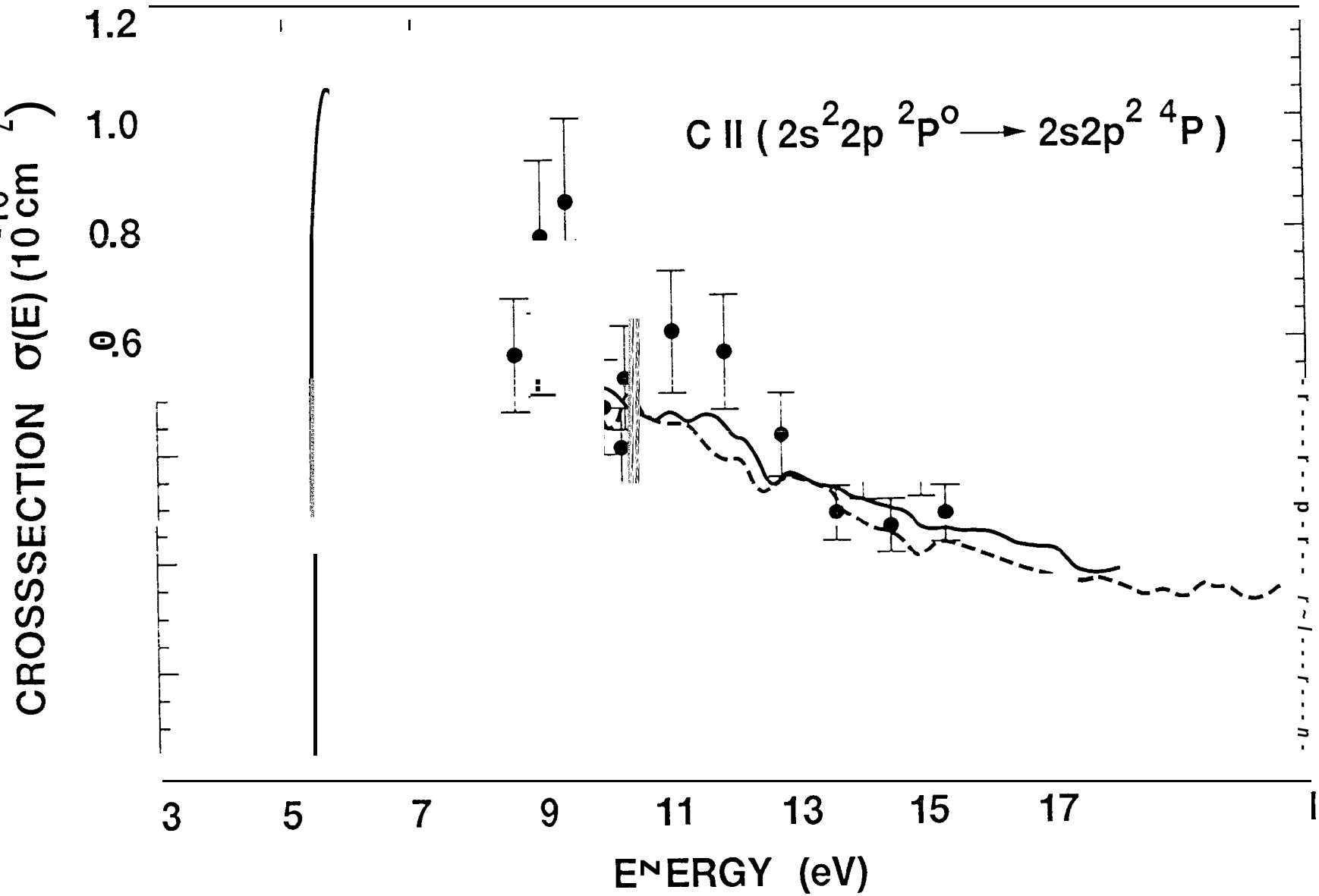
C II (2s²2p ²P° → 2s2p² ⁴P)
CROSSSECTION σ(E) (10⁻¹⁶ cm²)
1.2
1.0
0.8
0.6
3
5
7
9
11
13
15
17
ENERGY (eV)

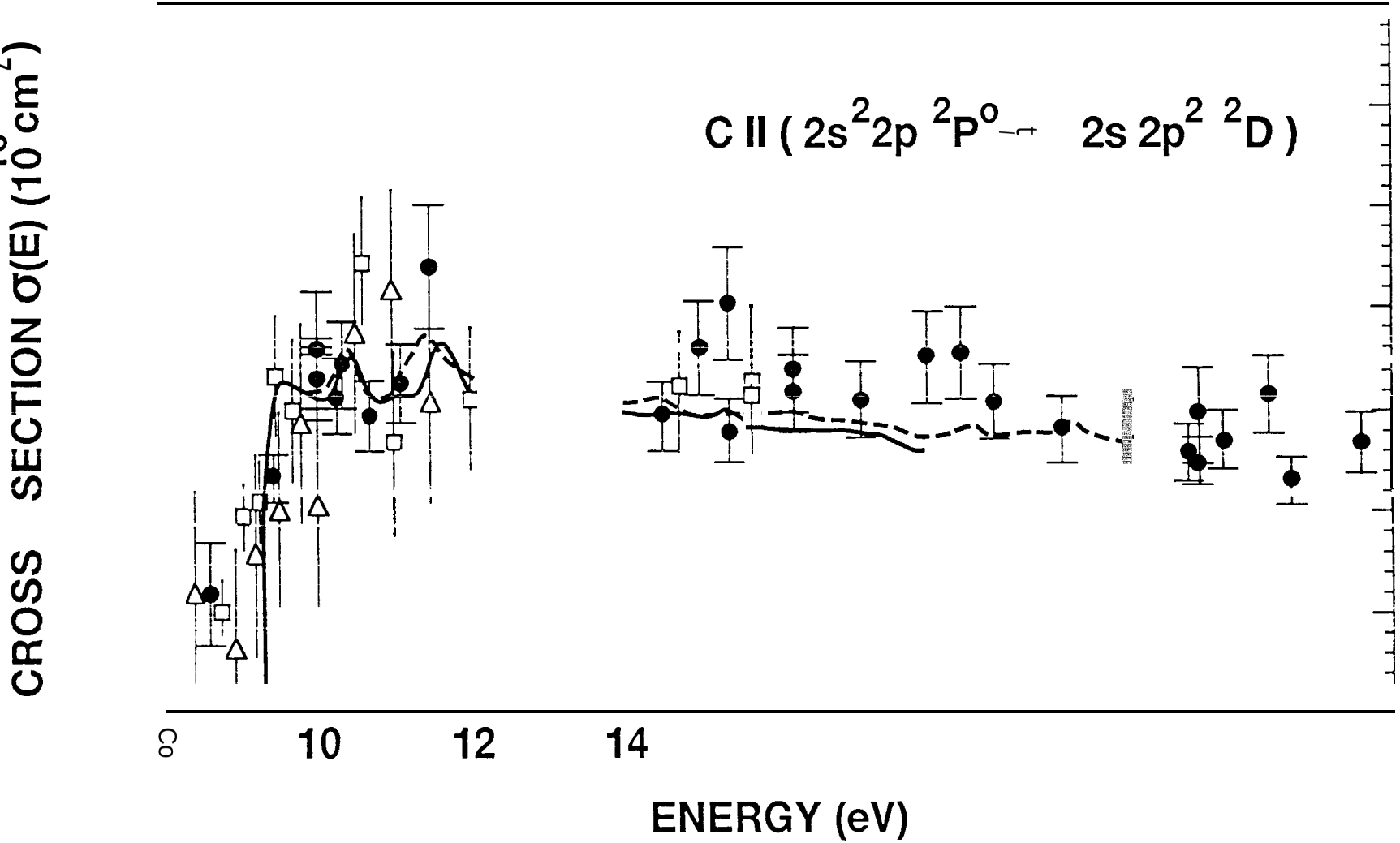
CROSS SECTION σ(E) (10^{-16} cm^2)
C II ($2s^2 2p\ ^2P^o$ – $2s\ 2p^2\ ^2D$)
0
10
12
14
ENERGY (eV)

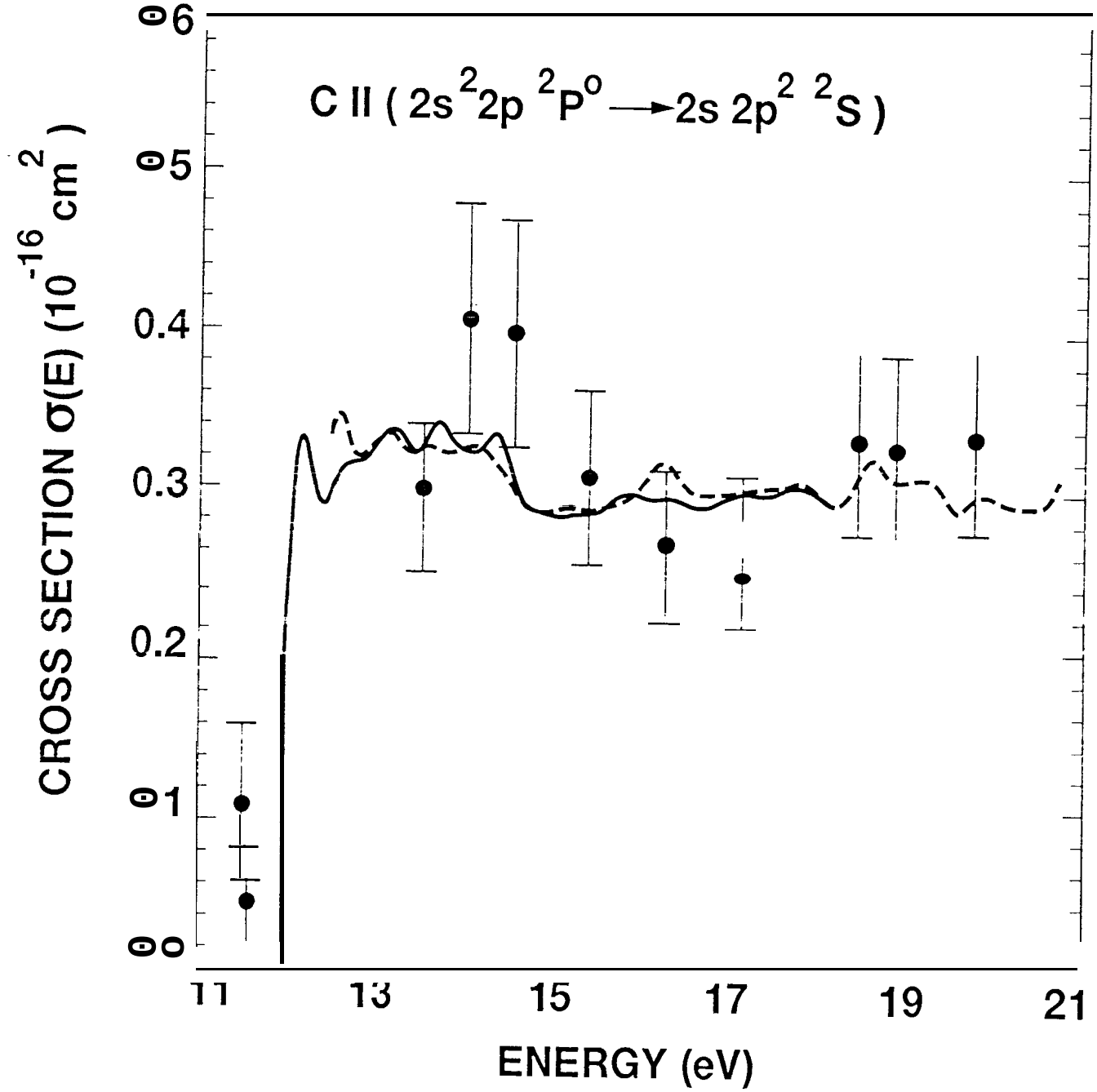
C II (2s 2 2p 2 P o → 2s 2p 2 2 S)
CROSS SECTION σ(E) (10 -16 cm 2)
0.6
0.5
0.4
0.3
0.2
0.1
0.0
11
13
15
17
19
21
ENERGY (eV)